Butti *et al.*
Journal of Electrical Systems and Inf Technol (2023) 10:29
https://doi.org/10.1186/s43067-023-00097-y

Journal of Electrical Systems and Information Technology

RESEARCH Open Access

An improved whale optimization algorithm for the model order reduction of large-scale systems

Dasu Butti[1*], Sivakumar Mangipudi[1], Srinivasarao Rayapudi[2], Madhu Kiran Buddi[1], Kalyan Raj Kaniganti[1], Trinayani Chittajallu[1], Bhavana Rushi Dontu[1], Vijay Arun Dunna[1], RamaKrishna Boni[1] and Chenchu Kishore Kumar Kothuri[1]

*Correspondence: dasu.geceee@gmail.com

[1] Department of EEE, Gudlvalleru Engineering College, Krishna (Dt.), Gudlavlleru, Andhra Pradesh, India 521356
[2] Department of EEE, University College of Engineering, JNTUK, East Godavari(Dt.), Kakinada, Andhra Pradesh, India 533001

Abstract

An improved whale optimization algorithm (IWOA) is developed for the model order reduction (MOR) of large-scale systems (LSS) in this paper. An equivalent reduced order model (ROM) for the higher-order system (HOS) is derived by considering integral square error (ISE) as the objective function using IWOA. Many practical systems of single-input and single-output (SISO) and multi-input and multi-output (MIMO) systems are considered to examine the worth of the proposed technique. The powerfulness and robustness of the proposed design technique are tested on various typical examples. Several simulation results have been reported to demonstrate the efficacy of IWOA. To prove the potentiality of the suggested technique, the results have been compared with the familiar classical MOR techniques as well as other heuristic algorithms available in the literature.

Keywords: Improved whale optimization algorithm, Large-scale systems, Model order reduction, Integral square error

Introduction

Usually, LSS when modeled will turn out into HOS because of large parameters involvement. Analysis of such HOS is tedious, complex, time-consuming, costlier, and requires more storage capacity. Over the last few decades, MOR techniques are developed to address the above issues. Hence, MOR techniques have been paid much attention in the field of control engineering to simplify large-scale practical systems like nuclear reactors, jet air engines, boilers, and generators connected to infinite bus systems. The biggest advantage of the MOR technique is the developed ROM provides the same behavior as its original HOS. Many MOR techniques have been proposed by several researchers in both time and frequency domains. The benchmark method that was developed by using Routh's table is presented in [1]. This method was realized as the prominent MOR technique in the field of control systems and it states that the ROM derived from the HOS is always stable when the original HOS is stable, and ROM can also be derived by using impulse energy approximation. Later, another method that uses both Routh's table

Springer Open

© The Author(s) 2023. **Open Access** This article is licensed under a Creative Commons Attribution 4.0 International License, which permits use, sharing, adaptation, distribution and reproduction in any medium or format, as long as you give appropriate credit to the original author(s) and the source, provide a link to the Creative Commons licence, and indicate if changes were made. The images or other third party material in this article are included in the article's Creative Commons licence, unless indicated otherwise in a credit line to the material. If material is not included in the article's Creative Commons licence and your intended use is not permitted by statutory regulation or exceeds the permitted use, you will need to obtain permission directly from the copyright holder. To view a copy of this licence, visit http://creativecommons.org/licenses/by/4.0/.

and Pade approximation is proposed in [2]. This model gives exact approximations without altering the characteristics of the original HOS of both SISO and MIMO systems. After that, a paper that describes a detailed narration of the MOR is outlined in [3]. The authors in [4] proposed a method in which the reduced transfer function of the HOS is determined from the Routh stability array by using an eighth-order model. Later, an improved version of the Pade approximation is depicted in [5, 6]. A paper that focuses on the derivations of transfer functions from the HOS is presented in [7]. A hybrid method of using Routh's stability equation method and Pade approximation is proposed in [8] which is simple and gives effective ROM for nonlinear systems also. In addition to the above, several classical MOR techniques [9–22] are reported in the literature. The application of MOR techniques to various practical systems is explored in [23–27]. However, involvement of more mathematical calculations, complexity and time consummation are the major drawbacks observed in classical techniques. In recent years, bio-inspired algorithms have emerged as powerful tools for solving complex problems. They were proven to address the issues listed above. Many heuristic algorithms are developed for the MOR techniques. Particle Swarm Optimization (PSO) [28, 29], Differential Evolution (DE) [30], Cuckoo Search Algorithm (CSA) [31,32, 33], Fire-Fly Algorithm (FFA) [33], Bat Algorithm (BA) [34], Big-Bang Crunch Algorithm (BBCA) [35], Enhanced DE[36, 37], PSO-DV[38] are some of the algorithms that are developed for the MOR. Though several methods are available, yet, an effective MOR technique for complex large-scale practical systems is still indispensable for getting the robust operation. Moreover, the above methods suffer from various drawbacks like premature convergence, not having good balance between exploitation & exploration stages, involvement of more design parameters, and steps that makes the optimization process complex and fails in evolving global best solutions. This motivates the authors to propose an effective method to address the above issues. Recently, IWOA [39] is proven its potential in solving complex engineering problems and addressed majority of the issues mentioned above. Hence, IWOA is considered to derive the ROM of some complex LSSs. The remainder of the paper is as follows. The second section depicts the statement of the problem, while the third section illustrates an overview of WOA. The fourth section explains the proposed IWOA for MOR and the performance analysis of IWOA on the test functions of CEC14 and CEC17. The fifth section presents the simulation results of three examples and the conclusion part is given in section six.

Problem statement

In this work, the authors considered some of the practical LSSs as examples to test the worth of the proposed IWOA method. The power system formulated by a modified single generator connected to an infinite bus system popularly known as Single Machine Infinite Bus System (MSMIB) and an air core of the transformer has been considered as the practical test examples to test the proposed IWOA technique. The MSMIB system is realized as a MIMO system, and the air core transformer linear section is realized as a SISO system. The IWOA is used to determine the coefficients of ROM of original higher-order MIMO and numerator and denominator coefficients of original higher-order SISO systems. Both the SISO and MIMO systems are represented as given below.

Consider a nth- order SISO can be represented by

$$G_n(s) = \frac{Y(s)}{U(s)} = \frac{\sum_{i=0}^{n-1} a_i s^i}{\sum_{j=0}^{n} b_j s^j} \tag{1}$$

where the order of numerator and denominator polynomial are $i = 0,1,2,3,....n\text{-}1$ & $j = 0,1,2,3,....n$, respectively. The equivalent r *th* $(r < n)$ ROM order to be derived, is represented by

$$R_r(s) = \frac{Y_r(s)}{U_r(s)} = \frac{\sum_{i=0}^{r-1} c_i s^i}{\sum_{j=0}^{r} d_j s^j} \tag{2}$$

where the order of numerator and denominator polynomial are $i = 0,1,2,3,....r\text{-}1$ & $j = 0,1,2,3,....r$, respectively. And any MIMO plant, G having the order of $n < \infty$, can be described by set of equations

$$\dot{X} = \mathrm{AX} + \mathrm{BU} \tag{3}$$

$$Y = \mathrm{CX} + \mathrm{DU} \tag{4}$$

where A is $m \times m$, B is $m \times 1$, C is $m \times r$, and D is $m \times m$ matrices, respectively.

The equivalent ROM of the original MSMIB system is assumed as G_r, having the order of $n_r < n$. The ROM to be determined has the same features as G, represented by the set of equations

$$\dot{X_r} = A_r X_r + B_r U \tag{5}$$

$$Y_r = C_r X_r + D_r U \tag{6}$$

where A_r is $r \times r$ matrix, B_r is $r \times 1$ matrix, C_r is $1 \times r$, D_r is $r \times r$ matrices of the ROM.

Overview of WOA

The WOA [40] was developed in the year 2016 after seeing the attacking behavior of the Humpback whales. These whales attack the prey in a nine-shaped path known as a bubble-net feeding mechanism. The whale generates a lot of bubbles along the nine-shaped path to form a net-type configuration to reach the target. The WOA is simple to understand and easy for the development of coding. The number of design parameters is less when compared to other algorithms. The rate of convergence is fast and takes minimum simulation time for getting optimum solutions (Fig. 1).

Steps involved in the WOA algorithm

Initially, initial parameters like population size, maximum iterations, minimum and maximum values of control variables, and other parameters of WOA are selected. Here, the ROM coefficients are considered as control variables. The initial solutions are generated randomly on a given objective function. The following steps depict various steps involved in determining the optimum solutions using WOA.

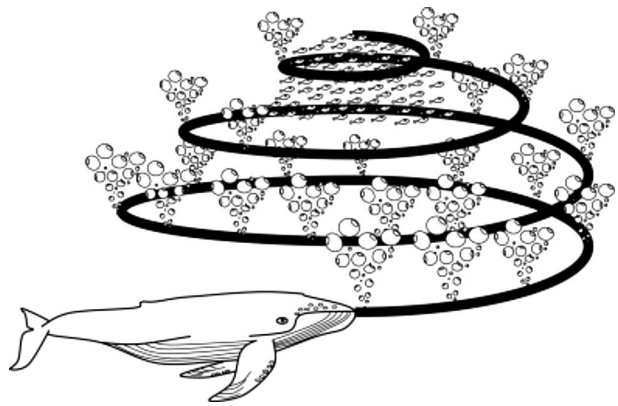

Fig. 1 The hunting strategy of Humpback Whales

Step 1 A Shrinking encircle mechanism for the position update of hunting agent As the initial solutions are generated randomly, the current solutions are considered as best solutions and the position of the whale is updated by using this mechanism. To attack the target, the whale follows a path which is defined by the equation below.

$$\vec{S} = R = R\ \vec{P} * (t) - \overrightarrow{P(t)} \tag{7}$$

$$\vec{P}_{(t+1)} = \vec{P}^{*}(t) - A\ \vec{S} \tag{8}$$

All the hunting agents change their position by using the above equations. Here, $\vec{S}$ depicts the distance between the whale and the target, R and A are the random numbers that are varied randomly during the optimization process, t be the current iteration, P^* corresponding to the optimum solution attained until now, $\vec{P}$ stands for the position vector, represents the absolute value. Here,A R are characterized as

$$A = 2ar - a \tag{9}$$

$$R = 2r \tag{10}$$

Here,A is the arbitrary number that alters between 2 and 0 and r is an arbitrary number that varies between (0,1). In every iteration process, the values of a, A, R are updated for each hunting agent. The present hunting agents update their location by Eq. 7 if the value of A is less than 1, and they follow the below equation otherwise.

$$S = R\ \vec{P}_{\text{rand}} - \vec{P} \tag{11}$$

$$\vec{P}(t+1) = \vec{P}^{*}(t) - A\vec{S} \tag{12}$$

where $\vec{\mathrm{P}}_{\text{rands}}$ is the random position vector which is selected in during the process from the present populations?

Step 2 A spiral mechanism for the position update of the hunting agent.

Hunting agents or ROM coefficients follow both shrinking cycle and spiral-shaped path during the search for their prey. To simulate the spiral-shaped track between the whale and target, a spiral equation is formulated. All the hunting agents update their position based on the formulated equation given below.

$$\overrightarrow{P}(t+1) = \overrightarrow{S}\, e^{bl} \cos(2\pi l) + \overrightarrow{P}^{*}(t) - A\,\overrightarrow{S} \tag{13}$$

where

$$\overrightarrow{S} = \overrightarrow{P}^{*}(t) - \overrightarrow{P}(t) \tag{14}$$

Here *'l'* is a stochastic limit that diverges between 0 and 1. Both spiral itinerary and spiral itinerary are merged by giving a 50% probability to both of them to update the positions. Finally, all the hunting agents follow the path described by the equation below.

$$\vec{P}(t+1) = \begin{cases} \vec{P}^{*}(t) - A\vec{S} & if\ \delta < 0.5 \\ \vec{S}e^{bl}\cos(2\pi l) + \vec{P}^{*}(t) - A\vec{S} & f\delta \geq < 0.5 \end{cases} \tag{15}$$

where δ is an arbitrary value that alters between 0 to 1.

IWOA for the MOR

The exploration and the exploitation stages are two important phases of any heuristic search algorithm. Maintenance of a good balance between these stages finds global solutions for complex engineering problems. Every particle finds a local best solution in the exploitation stage and a global best solution in the exploration stage. S. Mirjalili who developed the WOA has mentioned in his recent paper [31] that WOA fails to find the global optimum solutions as the solution to be updated in WOA for the next iteration depends upon the previous solution or current best solution. If the obtained current solution is not found to be the best solution, then the remaining solutions follow the current solution, and then there may be a chance of failure of getting global solutions. It is also mentioned that by improving the exploitation rate of the WOA, the strength of WOA could be improved. The convergence rate of WOA depends upon the best solutions attained so far. Hence, if the current best solutions obtained so far are not accurate then the algorithm may fail to find the global best solutions. This is the major disadvantage of the WOA. To address these issues, IWOA has been developed in this paper. In the IWOA, a weighting factor is added to the updating agent to accelerate the exploitation rate of the algorithm and thence to get the improvement in searching capability. The value of this factor is selected in such a way that it varies between 0.9 and 0.4 during the optimization process. The key function of the factor is to control the current best solutions so that they do not fall in local optima. It provides a good equilibrium between the stages of both exploration and exploitation. And finally, the algorithm can find the global optimum solutions. It was the change done to the WOA to attain IWOA. All the hunting agents update their positions using the following equations.

$$\overrightarrow{S} = Rw\overrightarrow{P}^*(t) - \overrightarrow{P}(t) \tag{16}$$

$$\overrightarrow{P}(t+1) = w\overrightarrow{P}^*(t) - A\overrightarrow{S} \tag{17}$$

Here, w is the weighing factor which is described as,

$$\begin{cases} w = \beta + \alpha \times \text{rand}\ (0,1) \\ \beta = \beta_{\min} + (\beta_{\max} - \beta_{\min}) \times \text{rand}\ (0,1) \end{cases} \tag{18}$$

where $\beta_{\min}$, $\beta_{\max}$ and β are the lower, upper, and mean values of the weighing factor. Here, α represents a constant number and the value is selected as 0.4 and *rand* is a numeral value that alters between 0–1 arbitrarily. During the optimization process, the hunting agents get minimum and maximum values of weights to fiddle with the weighting factor for the global optimization process. The spiral mechanism for the IWOA is modeled as

$$\vec{P}(t+1) = \vec{S}e^{bl}\cos(2\pi l) + w\vec{P}^*(t) - A\vec{S} \tag{19}$$

$$\text{Where } \overrightarrow{S} = w\overrightarrow{P}^*(t) - \overrightarrow{P}(t) \tag{20}$$

In the IWOA, the whales update their positions by following both shrinking encircle and spiral mechanisms to reach the target mechanism. Hence, to account for this, a 50% probability has been assigned to both the mechanisms. The whales update their positions by using the below equation if A is < 1; otherwise, they update their positions by using Eq. 11.

$$\overrightarrow{P}_{(t+1)} = \begin{cases} \{w\overrightarrow{P}^*(t) - A\overrightarrow{S} & if\ \delta < 0.5 \\ \overrightarrow{S}\,e^{bl}\cos(2\pi l) + w\overrightarrow{P}^*(t) - A\overrightarrow{S} & if\ \delta \geq < 0.5 \end{cases} \tag{21}$$

Performance analysis of IWOA

Before deriving the ROMs, the worth of IWOA is tested with the standard benchmark test functions of CE14 and CEC17. These test functions are highly nonlinear and getting a minimum fitness value is a challenging task. A total of thirty-three test functions are considered and tested with IWOA. The IWOA is applied to all test functions to investigate its potential of the IWOA. The test results in terms of minimum fitness value for all the test functions are presented in Tables 1 and 2, respectively. The test results of CEC 14 and CEC17functions are displayed in Tables 1 and 2, respectively. The results are compared with PSO, DE, and WOA-based results to show the superiority of the proposed IWOA. It is observed from the results that the fitness values obtained for the functions $f_1(x)$, $f_2(x)$, $f_3(x,)$, $f_4(x,)$, $f_7(x)$, $f_8(x)$ of CEC14 and test functions $f_1(x)$, $f_3(x)$, $f_4(x)$, $f_5(x)$, $f6(x)$, $f_7(x)$, $f_9(x)$, $f_{10}(x)$, $F_{11}(x)$ *of* CEC17 are minimum in case of IWOA when compared to other algorithms. Hence, it is realized that the IWOA is succeeded in finding the optimum solutions for the majority of the test functions when compared to other algorithms. Therefore, IWOA is utilized to design the ROM coefficients for the HOSs.

Table 1 Test results of CEC14 test functions

S.No	Name of the function	Order of the function	IWOA	WOA	DE	PSO
			Fitness value			
1	High Conditioned Elliptic function	$f_1(x)$	**1.4715e−90**	3.5101 e −80	3.5632 e−04	1.6684 e−80
2	Bent Cigar Function	$f_2(x)$	**1.1345 e−104**	4.0897 e−88	3.3893 e−04	1.9313 e−15
3	Discuss function	$f_3(x)$	**1.4795 e−93**	1.7573 e−73	8.6146 e−13	3.1554 e−22
4	Rosenbrocks Function	$f_4(x)$	**1.0812 e−06**	1.1866 e−06	3.0034 e−03	1.6720 e−02
5	Ackley's Function	$f_5(x)$	**4.4409 e−14**	4.4409 e−14	4.4409 e−14	4.4409 e−14
6	Weierstrass Function	$f_6(x)$	**9.441375732422 e−03**	9.441375732713 e−03	9.441375732812 e−03	9.441375733129 e−03
7	Griewanks Function	$f_7(x)$	**2.2204 e−16**	4.6928 e−08	7.0573 e−07	4.2514 e−06
8	Rastrigin's Function	$f_8(x)$	**1.4970 e−86**	1.3548 e−80	5.6960 e−05	0.001.2 e−03
9	Modified Schwefel's Function	$f_9(x)$	**0.0013**	0.0073	0.0038	0.0083
10	Katsuura Function	$f_{10}(x)$	**1.4746 e−11**	1.7937 e−10	4.4305 e−10	1.7377 e−10
11	HappyCat Function	$f_{11}(x)$	**3.5338 e−05**	1.7126 e−04	0.9555	1.6875 e−08
12	HGBat Function	$f_{12}(x)$	**1.4610 e−06**	2.7428 e−06	2.5256 e−03	8.2076 e−04
13	Expanded Griewanks plus Rosenbrocks Function	$f13(x)$	25.312	63.6412	4.5131	7.9816
14	Expanded Schaffer's Function	$f14(x)$	**1.7 e−03**	0.009.7 e−03	0.006.5 e−03	5.32 e−02

Bold represent the best fitness Values

The flowchart for the IWOA to get ROMs is depicted in Fig. 2. The convergence plots of some of the test functions are shown in Figs. 3 and 4. From the plots, it is proven that the IWOA finds the optimum solutions when compared to other techniques.

Implementation of IWOA for the MOR

Here, IWOA is used to determine the elements of A_r, B_r, C_r, and D_r of the MHP model. The following are various steps involved to get ROM using Improved WOA.

Step1: Initialization The algorithm starts with the initialization process. Here, elements of the original HOSs are chosen as design parameters and are optimized to get desired ROM that preserves most of the dynamic behavior of the original HOS. Here, a fourth-order ROM is to be derived from their HOS using IWOA. The initial values of control variables are arbitrarily generated by using the expression given below.

$$Z_{i+1} = Z_i^{\min} + \text{rand}.(Z_i^{\min} - Z_i^{\max}) \tag{22}$$

Table 2 Test results of CEC17 test functions

S.No	Name of the function	Order of the function	IWOA	WOA	DE	PSO
			Fitness value			
1	Bent Cigar Function	$f_1(x)$	**1.1345 e−104**	4.0897 e−88	3.3893 e−04	1.9313 e−15
2	Sum of Differential Power Function	$f_2(x)$	**99.515675936657374**	99.515675945535875	99.5157	99.5157
3	Zakharov Function	$f_3(x)$	**3.2883e−111**	9.5876e−80	2.5150e−08	4.1649e−09
4	Rosenbrocks Function	$f_4(x)$	**1.0812e−06**	1.1866e−06	3.0034e−03	1.6720 e−02
5	Rastrigin's Function	$f_5(x)$	**1.4970 e−86**	1.3548 e−80	5.6960 e−05	0.001.2 e−03
6	Expanded Schaffers function	*f6(x)*	0.0017	0.0097	0.0065	0.0532
7	Lunacek bi-Rastrigin function	*f7(x)*	2.3231 **e−**09	2.7252 e−07	0.0373	0.1205
8	Levy Function	*F8(x)*	**70.1407e+00**	70.0737 e+00	70.3698e+00	78.0292e+00
9	Modified Schwefel's Function	$F_9(x)$	**3.0417e+06**	4.1183e+06	4.1479e+06	4.1482e+06
10	High Conditioned Elliptic function	$f_{10}(x)$	**1.4715 e−90**	3.5101 e−80	3.5632 e−04	1.6684 e−80
11	Discuss function	$F_{11}(x)$	**1.4795 e−93**	1.7573 e−73	8.6146 e−13	3.1554 e−22
12	Ackley's Function	$F_{12}(x)$	1.6556e+002	1.6556e+002	1.6587e+002	8.5076e+00
13	Weierstrass Function	$F_{13}(x)$	9.441375732422 **e−03**	9.441375732713 e−03	9.441375732812 e−03	9.441375733129 e−03
14	Griewanks Function	$F_{14}(x)$	9.8255 **e−**14	5.6654 e−08	0.3131 e−04	1.0852 e−07
15	Katsuura Function	$f_{15}(x)$	1.4746 **e−**11	1.7937 e−10	4.4305 e−10	1.7377e−10
16	HappyCat Function	$f_{16}(x)$	**3.5338 e−05**	1.7126 e−04	0.9555	1.6875 e−08
17	HGBat Function	$f_{17}(x)$	**1.4610 e−06**	2.7428 e−06	2.5256 e−03	8.2076 e−04
18	Expanded Griewanks plus Rosenbrocks Function	*f18(x)*	25.312	63.6412	4.5131	7.9816
19	Schaffer's function	*F19(x)*	**0.0010**	0.1606	0.0090	0.4613

Bold represent the best fitness Values

where Z defines the control variable which is to be updated in every iteration, *rand* is an arbitrary number that varies between 0 to 1. Here $Z_i^{\min}$ and $Z_i^{\max}$ are the minimum and maximum values of the control variables, respectively. The total number of iterations is taken as 100; population size is selected as 50.

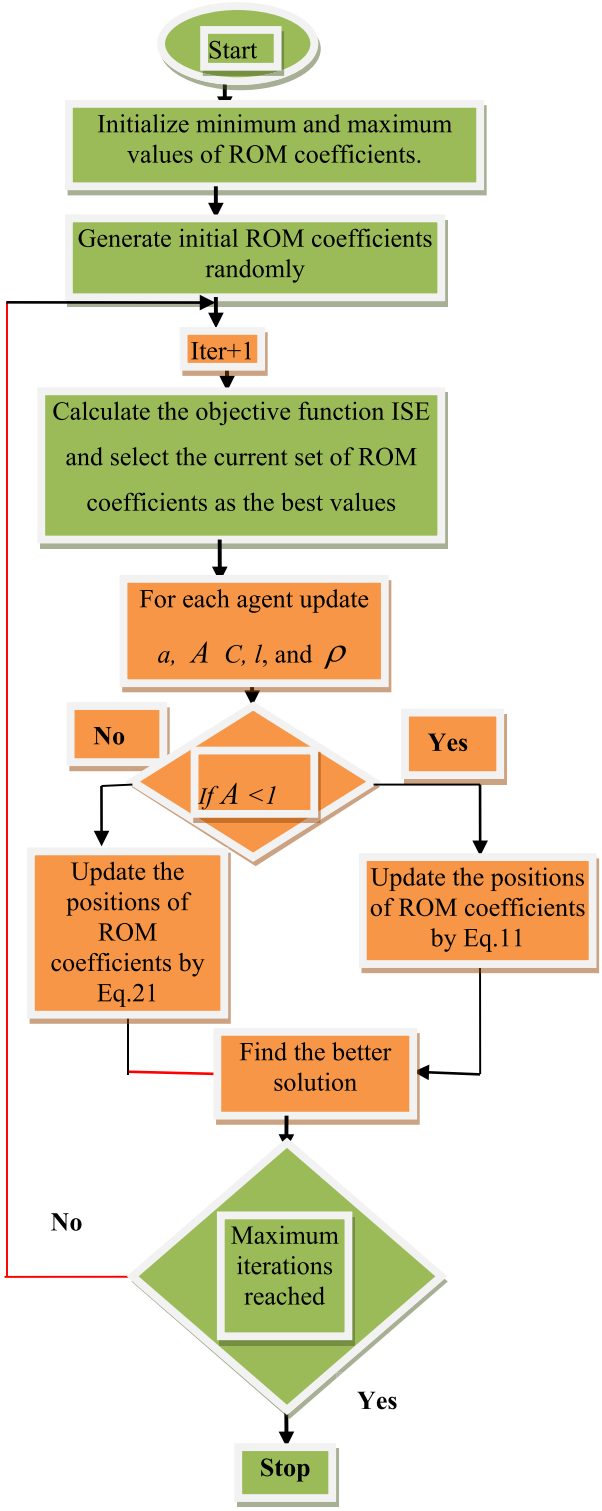

Fig. 2 Flowchart to determine the ROM coefficients

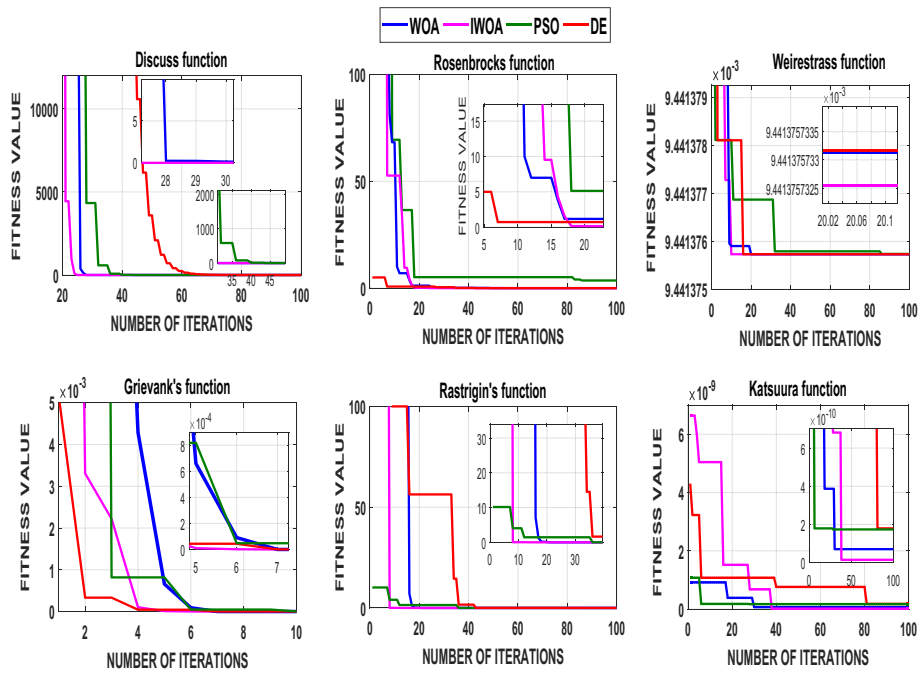

Fig. 3 Convergence plots of various CEC 14 test functions

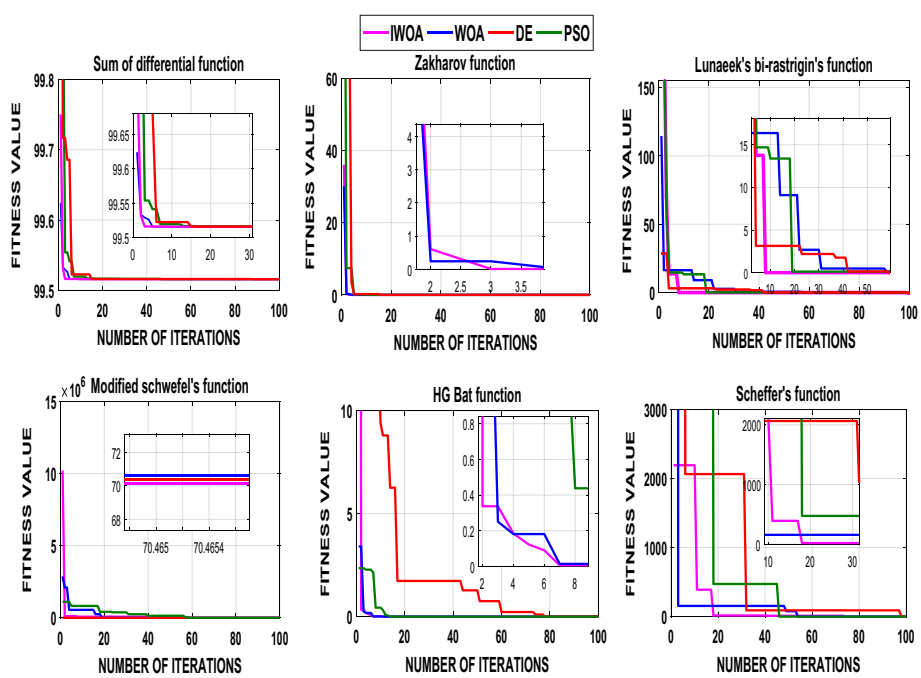

Fig. 4 Convergence plots of various CEC 14 test functions

Step 2 Evaluating the objective function.

Here, to determine the ROM coefficients of the MSMIB system, ISE is used as the objective function. The reason behind the selection of this function is it is the most

popular and efficient measure of the dynamic execution of the system. The below equation depicts the expression for ISE.

$$J_1 = \int_0^t (e)^2 = \int_0^t [y(t) - y_r(t)]^2 \tag{23}$$

Here, 'e' is the error between the step responses of the HOS and reduced order system (ROS). Here $y(t)$ and $y_r(t)$ are the step responses of the original HOS and ROMs, respectively. IWOA is used to minimize the objective function J_1 so that the derived ROM can retain the maximum dynamic response of the original HOS.

Step 3 Shrinking encircle mechanism for the position update of hunting agent.

Here, the ROM coefficients which are to be optimized are selected as search agents. All the ROM coefficients follow Eqs. 16–18 to update their positions.

Step 4 Spiral mechanism for the position update of the hunting agent.

All the ROM coefficients to be optimized follow Eqs. 19–20 to update their positions. IWOA has been run several times until the optimized ROM coefficients are obtained. Figure 2 shows the flow chart for IWOA to optimize the ROM coefficients.

Numerical examples and results

To investigate the performance of the proposed IWOA-based MOR technique, three practical examples are considered; out of them, two are SISO systems and one is a practical MIMO system (MSMIB system).

Example 1 single input single output (SISO) system

To start with, a seventh-order HOS is taken as one of the test examples collected from the literature. Here, the coefficients of the numerator and denominator of the HOS are assigned as the tunable elements to minimize the fitness function. The boundary values of tunable elements are selected and the process of optimization is started with the generations of random solutions. The original HOS of the SISO system is given by

$$G_7(s) = \frac{\begin{array}{l} 2000s^6 + 121700s^5 + 1.21 \times 10^6 s^4 + 7.454 \times 10^6 s^3 + 5.527 \times 10^7 s^2 \\ +3.156 \times 10^7 s + 2.075 \times 10^6 \end{array}}{s^7 + 65.85s^6 + 984.2s^5 + 12130s^4 + 97300 + 429400 + 2.0188 \times 10^6 s + 999500} \tag{24}$$

The optimized second-order ROM of the original HOS by using IWOA is shown below..

$$R_2(s) = \frac{45s + 9.8332}{0.1s^2 + 0.035s + 3.712} \tag{25}$$

The second-order ROMs of classical methods are compared with the proposed IWOA-based ROM (IWOA-ROM) and are depicted in Table 3. The ISE values are also presented in the table. Table 3 represents the comparison of ROMs of classical and heuristic techniques with the proposed ROM.

Table 3 Comparison of ROMs with proposed IWOA

Name of the method	Reduced order model	ISE
IWOA	$\frac{45s+9.8332}{0.1s^2+0.035s+3.712}$	9.3080e + 03
WOA	$\frac{97.99s+30.08}{0.4792s^2+s+11.98}$	1.6 63e + 04
BAT [33]	$\frac{72.3394s+4.88324}{s^2+5.0995s+4.5278}$	1.7117e + 04
FFA [32]	$\frac{67.779s+4.5278}{s^2+5.0995s+2.3277}$	1.7204e + 04
DE [29]	$\frac{100s+100}{0.4068s^2+s+9.731}$	1.3323e + 04
PSO [28]	$\frac{100s+42.21}{0.403s^2+s+20}$	1.5409e + 04
C.B. Viswakarma [41]	$\frac{187s+12.64}{s^2+10.88s+6.087}$	1.5660e + 04
Jayantha Pal [6]	$\frac{2.938\times10^7s+2.075\times10^6}{5.533\times10^4s^2+1.139\times10^6s+9.995\times10^5}$	1.3125e + 04
Y Shamash [37]	$\frac{0.03787s+0.017346}{s^2+0.5462s+0.03591}$	1.8624e + 04
Seshadri et.al [4]	$\frac{1.13\times10^6s+999500}{2.355\times10^7s^2+3.144s+2.075\times10^6}$	1.8624e + 04
Routh approximation [1]	$\frac{81.98s+5.39}{s^2+5.684s+2.596}$	1.6959e + 04

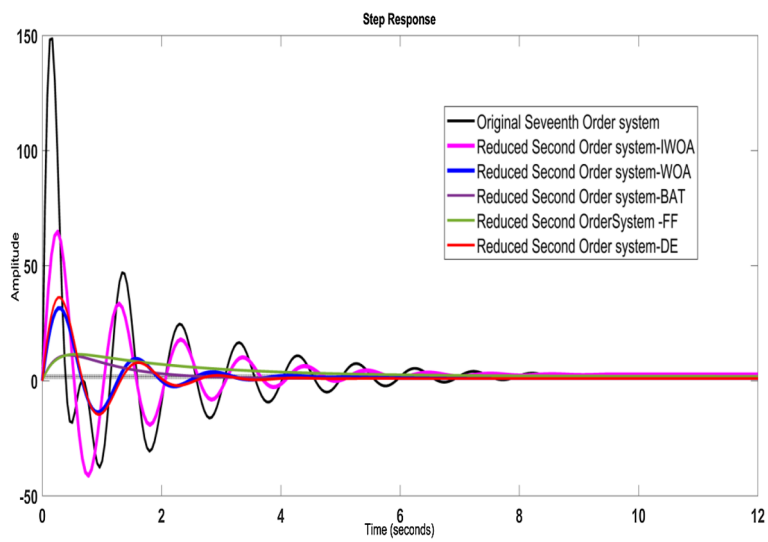

Fig. 5 Comparison of IWOA-ROM with ROMS of other techniques for the step input

The step responses of original HOS, IWOA-ROM and ROMs of other heuristic and classical techniques are depicted in Fig. 5. Figure 6 depicts the bode plot of original HOS, IWOA-ROM, and ROMs of other heuristic and classical techniques. From the simulation results, it is proven that the IWOA-ROM exactly matches with original HOS in the majority of the regions, i.e., at both transient and steady states. The phase margin and gain margin of the IWOA-ROM closely coincide with the original system when compared to other algorithms. Hence, it is observed that the IWOA gives optimum ROM than other techniques in both time and frequency domains. The convergence plots of the IWOA, WOA, DE, and PSO algorithms are shown in Fig. 7.

Example 2 To investigate the worth of the IWOA, here another example of a practical case study is considered. The linearized section of the air-core transformer, which consists of ten segments, is considered as a second example. The transfer function of the air core transformer is obtained as.

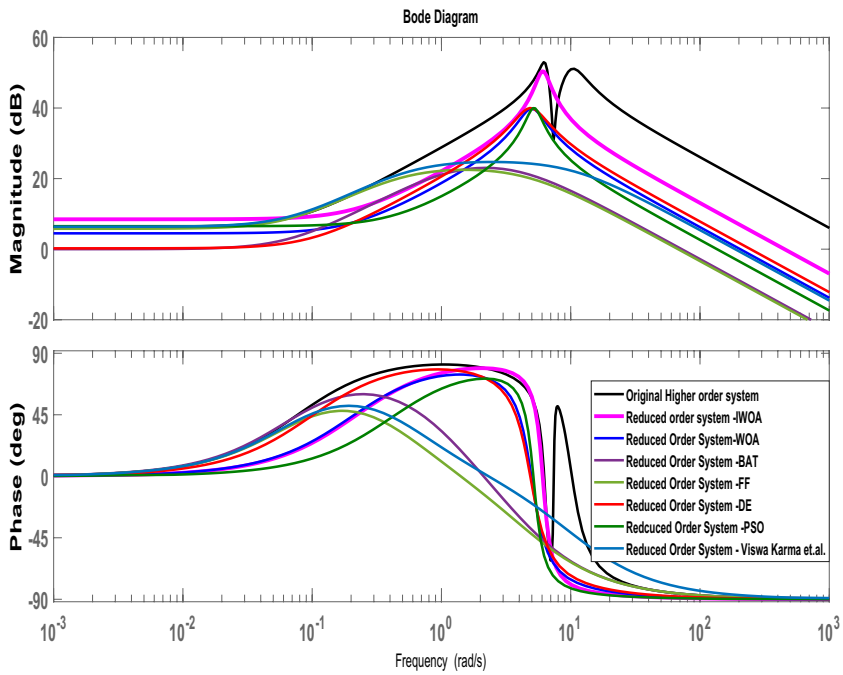

Fig. 6 Comparison of IWOA-ROMs with ROMs of other techniques with a bode plot

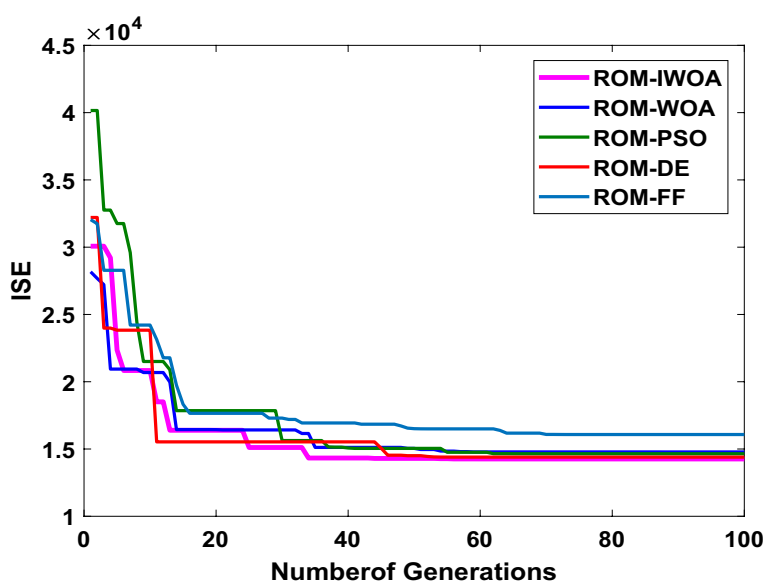

Fig. 7 Convergence plots of IWOA and other techniques

$$G(s) = \frac{(s^9 + 510.1s^8 + 1.106e5\, s^7 + 1.33\, e7\, s^6 + 9.691\, e8\, s^5 + 4.393\, e10\, s^4 + 1.223\, e12\, s^3 + 1.981\, e13\, s^2 + 1.652\, e13\, s + 5.211\, e14)}{(s^{10} + 529.8s^9 + 120200s^8 + 1.527\, e7\, s^7 + 1.191\, e9\, s^6 + 5.892\, e10\, s^5 + 1.842\, e12\, s^4 + 3.513\, e13\, s^3 + 3.784\, e14\, s^2 + 1.965\, e15\, s + 3.32\, e15)} \tag{26}$$

Table 4 Comparison of IWOA-ROMs with some familiar ROMs

#Method#	Reduced second-order system	ISE
IWOA	$R_2(s) = \frac{0.6318s+7.112}{0.6419s^2+16.58s+45.35}$	2.7330e−10
WOA	$R_2(s) = \frac{1.972s+28.25}{0.3372s^2+60s+180}$	3.1355e−9
DE[29]	$R_2(s) = \frac{1.977s+31.02}{0.291s^2+65s+197.7}$	5.7048e−09
PSO [28]	$R_2(s) = \frac{1.506s+31.39}{0.477s^2+65.24s+200}$	6.2590e−09
EDE [36]	$R_2(s) = \frac{0s+1568.5185}{s^2+6090.422363s+200}$	3.92e−04
EDE & Improved MMPA method [37]	$R_2(s) = \frac{0.400757s+200.396591}{s^2+780.5269s+1276.7544}$	4.016e−04
PSO-DV[38]	$R_2(s) = \frac{5.00995s+129.01962}{s^2+523.004761s+822.001831}$	4.1e−04
Sambapriya et.al [40]	$R_2(s) = \frac{0.8664s+7.328}{s^2+18.32s+46.83}$	3.32e−04
Pole cluster & Pade Approximation[22]	$R_2(s) = \frac{-18.77s+119.7}{s^2+90s+762.6}$	5.7586e−7
Srinivasan & Krishnan [42]	$R_2(s) = \frac{1.603s+27.57}{s^2+58.412s+175.96}$	3.7411e−6
C.B. Vishwakarma [41]	$R_2(s) = \frac{1.648s+29.92}{s^2+62.59s+190.64}$	9.7279e−9
Girish Parmar [43]	$R_2(s) = \frac{3.326s+48.3}{s^2+105.95s+308.159}$	2.4507e−6
Y Shamash [44]	$R_2(s) = \frac{0.5178s+1.633}{s^2+6.159s+10.41}$	2.2015e−07
Jayantha pal [6]	$R_2(s) = \frac{9.751e13s+5.211e14}{2.28e14s^2+1.53e15s+3.32e15}$	2.3303e−07
VV Seshadri [4]	$R_2(s) = \frac{0.5178s+1.633}{s^2+6.159s+10.41}$	2.2015e−07

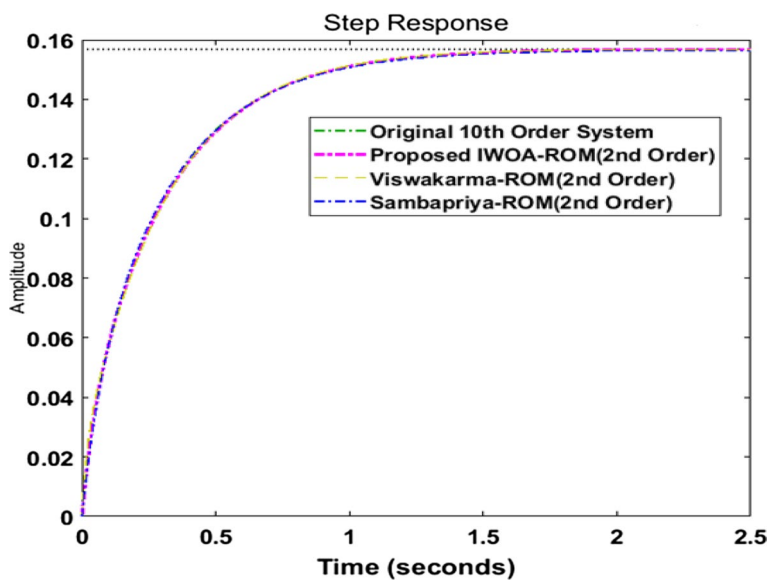

Fig. 8 Comparison of IWOA-ROM with ROMS of other techniques for the step input

The IWOA has been run several times until the optimized second-order ROM is attained. The optimized ROM in the second-order form using IWOA is depicted below.

$$R_2(s) = \frac{0.6318s + 7.112}{0.6419s^2 + 16.58s + 45.35} \tag{27}$$

The derived second-order IWOA-ROM is compared with other ROMs which were determined using WOA, DE, PSO, and classical methods that existed in the literature. The details of ROMs are reported in Table 4. Table 4 presents the comparison of the

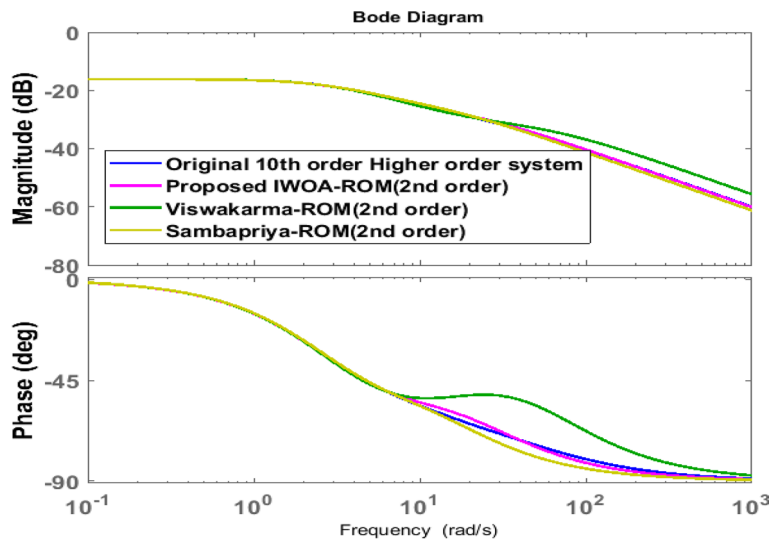

Fig. 9 Bode response comparisons of original HOS and Proposed ROMs

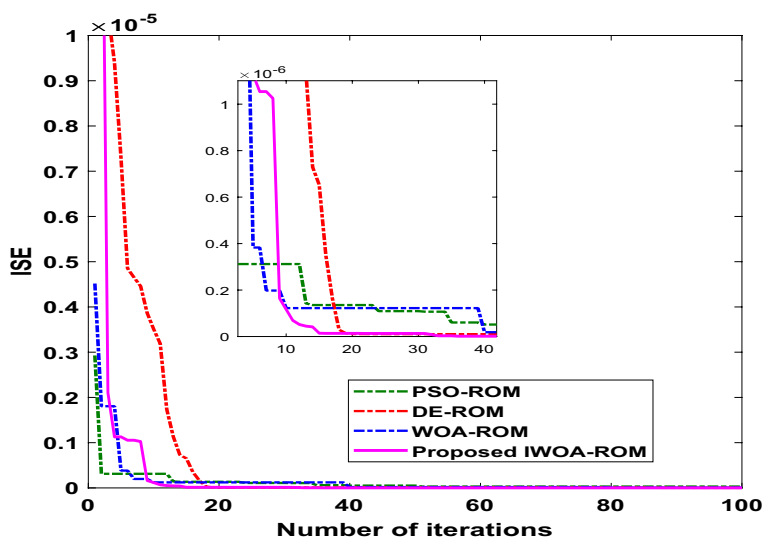

Fig. 10 Convergence plots of proposed and other algorithms

IWOA-ROM with the ROMs of the other techniques which are available in the literature. The ISEs of all the techniques are also depicted in the table. It is examined from the results that the IWOA-ROM has provided the smallest amount of ISE value when contrasted to other methods. The step responses of original tenth-order HOS, IWOA-ROM and other ROMs are shown in Fig. 8. It is proven from the responses that the proposed IWOA-ROM exactly matches with the original HOS at all the regions, i.e., at both transient and steady states. Hence, it can be concluded that the proposed IWOA has succeeded in finding an optimum ROM when compared to other techniques (Figs. 9 and 10).

Table 5 Operating conditions for MSMIB system

Loading condition	*P* (p.u)	*Q* (p.*u*)
1	1.1	0.5
2	0.8	0.4
3	0.4	0.1

Example 3 MSMIB system (MIMO system).

This MSMIB system gives the ninth order when it is modeled and is taken as the third example to derive its equivalent fourth-order ROM. The main objective of reducing the ROM into the fourth order is to retain the majority of the dynamic performance of the

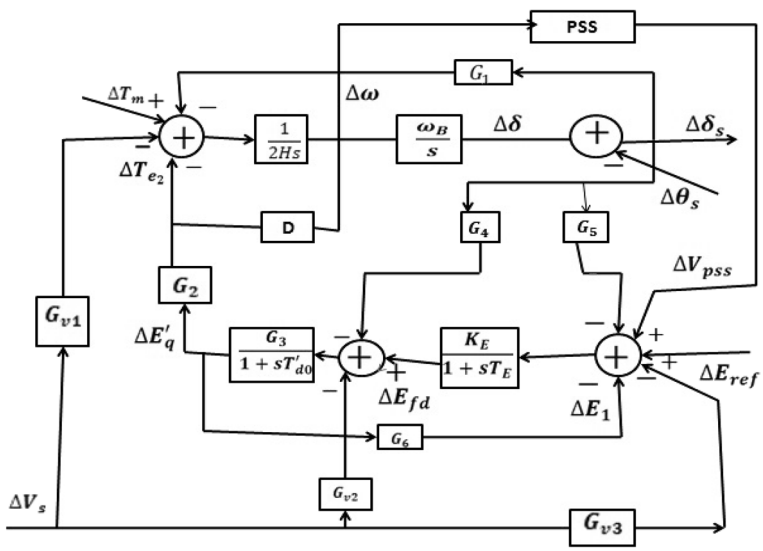

Fig. 11 The block diagram Heffron-Phillip's model

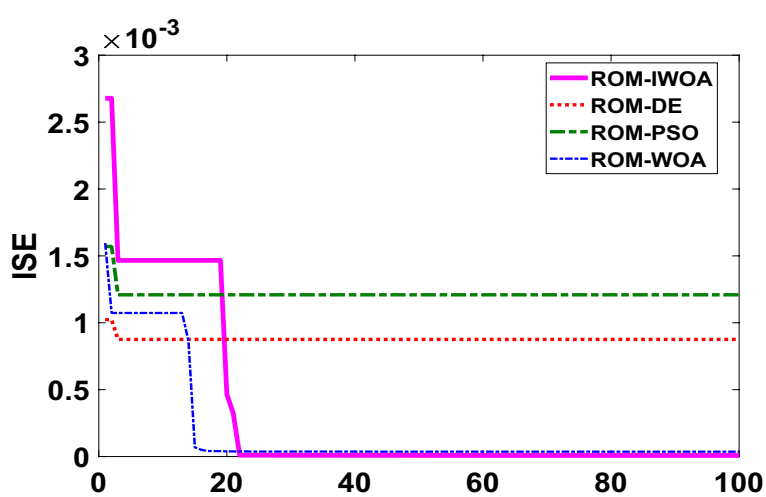

Fig. 12 Convergence plots of IWOA, WOA, DE, and PSO techniques

original HOS. Under this example, three typical operating conditions have been considered and subsequent ROMs are derived to examine the strength of the IWOA technique. Table 5 shows the operating conditions taken for deriving G-constants. The block diagram of the MHP model for the MSMIB system is depicted in Fig. 11. The MHP model is formulated using the G-constants, which can be determined from the following expressions (Fig. 12).

For any operating condition, the G-constants are represented as

$$G_1 = \frac{V_{s_o} E_{q_o} \text{si n}\delta_s}{X_q + X_t} + \frac{X_q - X'_d}{X_t + X'_d} V_s \sin\delta_s \tag{28}$$

$$G_2 = \frac{X_q + X_t}{X_t + X'_d} i_q \tag{29}$$

$$G_3 = \frac{X_t + X'_d}{X_d + X_t} \tag{30}$$

$$G_4 = \frac{X_d - X'_d}{X_t + X'_d} V_s E_q \text{si n}\delta_s \tag{31}$$

$$G_5 = \frac{X_q V_d V_s \cos\delta_s}{(X_q + X_t) V_t} - \frac{X'_d V_s \ \sin\delta_s}{(X_t + X'_d) V_t} \tag{32}$$

$$G_6 = \frac{X_t}{X_t + X'_d} \frac{V_q}{V_t} \tag{33}$$

$$G_{v_1} = \frac{E_{q_o} \sin\delta_s}{(X_t + X_q)} - \frac{(X_q - X'_d) I_q \cos\delta_s}{(X'_d + X_t)} \tag{34}$$

$$G_{v_2} = -\frac{(X_d - X'_d) \cos \delta_{s_o}}{(X'_d + X_t)} \tag{35}$$

$$G_{v_3} = \frac{X_q V_d \sin\delta_s}{X_q + X_t} + \frac{X'_d V_q \cos\delta_s}{(X_t + X'_d) V_t} \tag{36}$$

where $E_{q_o} = E'_{q_o} - (X_q - X'_d) i_d$. For any operating condition of the MSMIB system, V_S is the transformer secondary bus voltage, δ_s is the load angle measured to transformer secondary voltage,E'_q is the field flux transient emf, X_q is the reactance of q-axis, X_d is the reactance of d-axis, X'_d is the reactance of q-axis, i_d is the stator current of d-axis, i_q is the stator current of q-axis, E_{fd} is the field voltage, T_e is the time constant of exciter, K_e is gain of exciter, V_{ref} is the reference voltage, V_{pss} is the input of the PSS, V_t is the terminal voltage of the generator, X_t is the reactance of the transformer. The K-constants for the three operating conditions are determined by using the above expressions and listed in

Table 6 *K*- constants for operating conditions of MSMIB system

Operating Point	K_1	K_2	K_3	K_4	K_5	K_6	KV_1	KV_2	KV_3
1	2.1697	1.0013	0.3429	1.4147	− 0.038	0.5842	0.4562	− 1.29	0.6507
2	1.9788	0.8945	0.3429	1.2714	0.0092	0.5593	0.2429	− 1.43	0.6061
3	1.6077	0.7416	0.3429	1.0686	0.0642	0.4979	− 0.005	− 1.59	0.5229

Table 7 Optimized IWOA-ROMs in state space representation

Loading condition	A_r	B_r	C_r	D_r
1	$\begin{bmatrix} 0 & 0 & 0 & 0 \\ -681 & 0 & 0 & 0 \\ 1967 & 877 & -20 & -31217 \\ 0 & 1 & 0 & -46 \end{bmatrix}$	$\begin{bmatrix} 0 \\ 2.1697 \\ -6.2653 \\ 0 \end{bmatrix}$	$\begin{bmatrix} 314 & 0 & 0 & 0 \\ 0 & 0 & 0 & 0 \\ 0 & 0 & 0 & 0 \\ 2412 & 877 & -19 & -31217 \end{bmatrix}$	$\begin{bmatrix} -1.000 \\ 0 \\ 0 \\ -7.6800 \end{bmatrix}$
2	$\begin{bmatrix} 0 & 0 & 0 & 0 \\ -621 & 0 & 0 & 0 \\ -977 & 1256 & -19 & -26970 \\ 0 & 2 & 0 & 46 \end{bmatrix}$	$\begin{bmatrix} 0 \\ 1.9788 \\ 3.114 \\ 0 \end{bmatrix}$	$\begin{bmatrix} 314 & 0 & 0 & 0 \\ 0 & 0 & 0 & 0 \\ 0 & 0 & 0 & 0 \\ -578 & 1256 & 19 & -6970 \end{bmatrix}$	$\begin{bmatrix} -1.000 \\ 0 \\ 0 \\ 1.8400 \end{bmatrix}$
3	$\begin{bmatrix} 0 & 0 & 0 & 0 \\ -681 & 0 & 0 & 0 \\ 1967 & 1200 & -20 & -36000 \\ 0 & 1 & 0 & -20 \end{bmatrix}$	$\begin{bmatrix} 0 \\ 2.1697 \\ -6.2653 \\ 0 \end{bmatrix}$	$\begin{bmatrix} 314 & 0 & 0 & 0 \\ 0 & 0 & 0 & 0 \\ 0 & 0 & 0 & 0 \\ 2412 & 1200 & -19 & -36000 \end{bmatrix}$	$\begin{bmatrix} -1.000 \\ 0 \\ 0 \\ -7.6800 \end{bmatrix}$

Table 6. Table 6 shows the G-constants determined for the considered operating conditions. Using the K- constants and the machine data, the state space representations of the MHP model for all three operating conditions have been derived and are shown in Appendix. The fourth-order ROMs of HOS in state space for three operating conditions using the IWOA technique are represented form in Table 7. Table 7 depicts the state space representation of IWOA-ROMs.Comparison plots of HOS and ROM for IWOA, WOA, DE, and PSO-based algorithms for the three loading conditions are shown in Fig. 13. Plots displayed in Fig. 13a–c) give the step responses of the loading condition. Plots in Fig. 13d–f depict the step responses of loading condition 2, and the plots for the third loading condition are shown in Fig. 13g–i. The dark blue color depicts the response of the original HOS for the step input, the pink color stands for the response of IWOA-ROM for the step input, the red color plot gives the step response of the WOA-ROM, and the green color corresponds to the response of the PSO-ROM for the step input. All step responses are compared on a common time scale to test their performances. Simulation results clearly show that the behavior of the ROM obtained from IWOA closely matches the behavior of the original HOS when compared to the other ROMs at transient and steady-state conditions for loading condition one. Similarly, ROMs second and third loading conditions also exhibited the same type of performance when compared to the other algorithms. Hence, it is concluded from the results that the ROMs

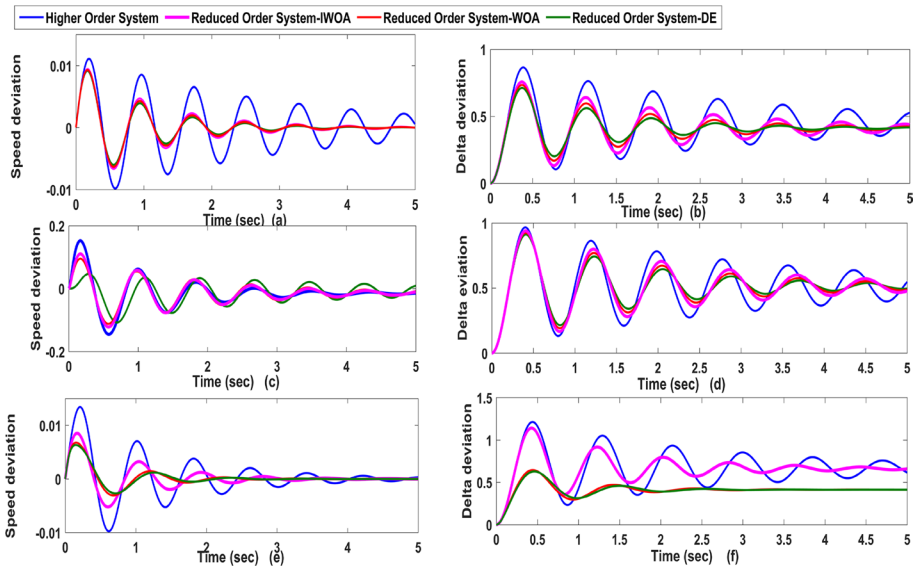

Fig. 13 Step response comparisons of original HOSs and ROMs for the three Step loading conditions

derived from the IWOA technique retain most of the dominant behavior of its original higher-order plant at all the loading conditions when compared to the ROMs derived from WOA, DE, and PSO algorithms.Further, to show the efficacy of the proposed work, bode plots of the obtained ROMs and the original HOSs are shown in Figs. 14, 15 and 16. Plots of four important states: $\Delta\delta$, $\Delta\omega$, ΔEq, ΔE_{fd} of original HOS and ROMs are presented in the figures. The black color plot represents the response of the original ninth-order MSMIB system, the dark pink color represents the response of the proposed IWOA-ROM, the blue color plot represents the response of the WOA-ROM, the red color plot depicts DE-ROM and the response of PSO- ROM is represented in green color. The results prove that the phase margin and gain margins of the proposed IWOA-ROM of four states match with the original HOSs' states in a better way when compared to other ROMs.

Conclusions

IWOA-based MOR technique is proposed on three typical complex LSSs. ISE is considered as an objective function to optimize the coefficients of ROMs of the original HOS systems. SISO and MIMO systems are considered to study the comparative analysis. The MHP model, which is having ninth order, air core of the transformer of the order of tenth order, and seventh-order systems are taken as test cases to examine the performance of the proposed IWOA-based MOR technique. Performance of the ROMs derived using WOA, DE, and PSO and other classical techniques has been contrasted with IWOA- ROM. The test results conclude that the IWOA-ROM exhibited better performance when compared to other methods.

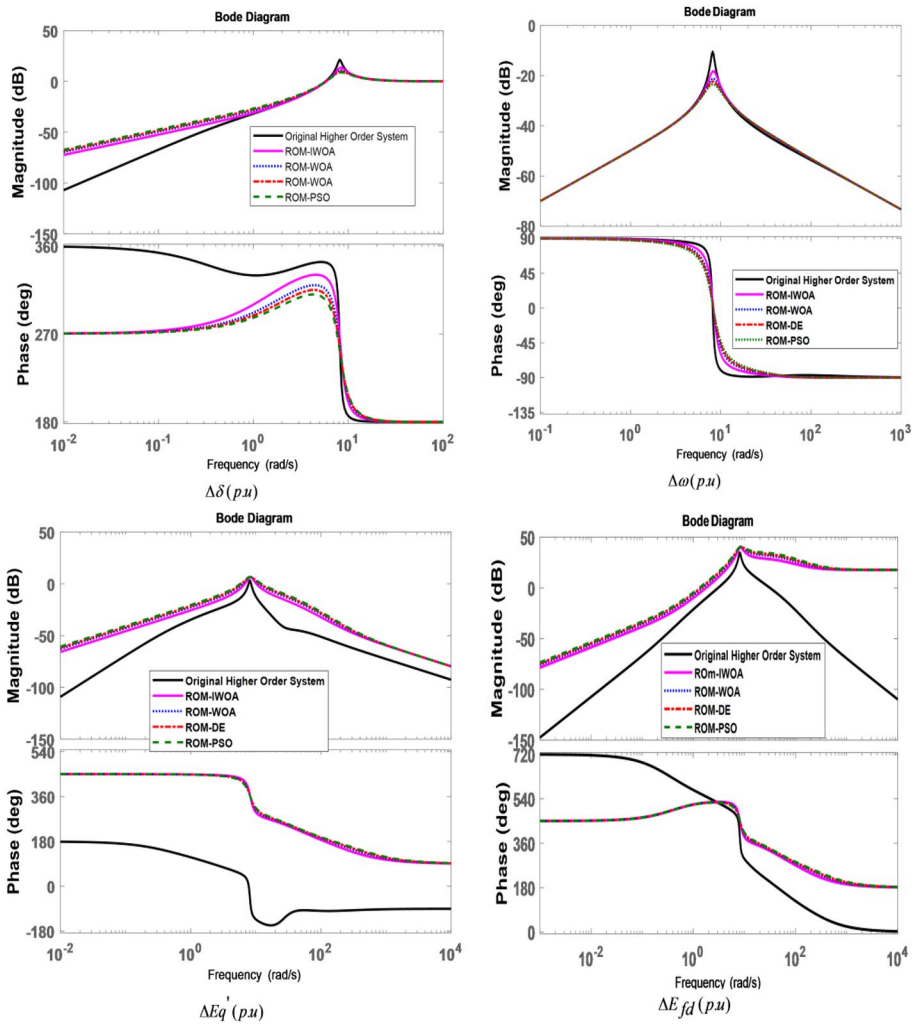

Fig. 14 Bode plot responses of loading condition 1

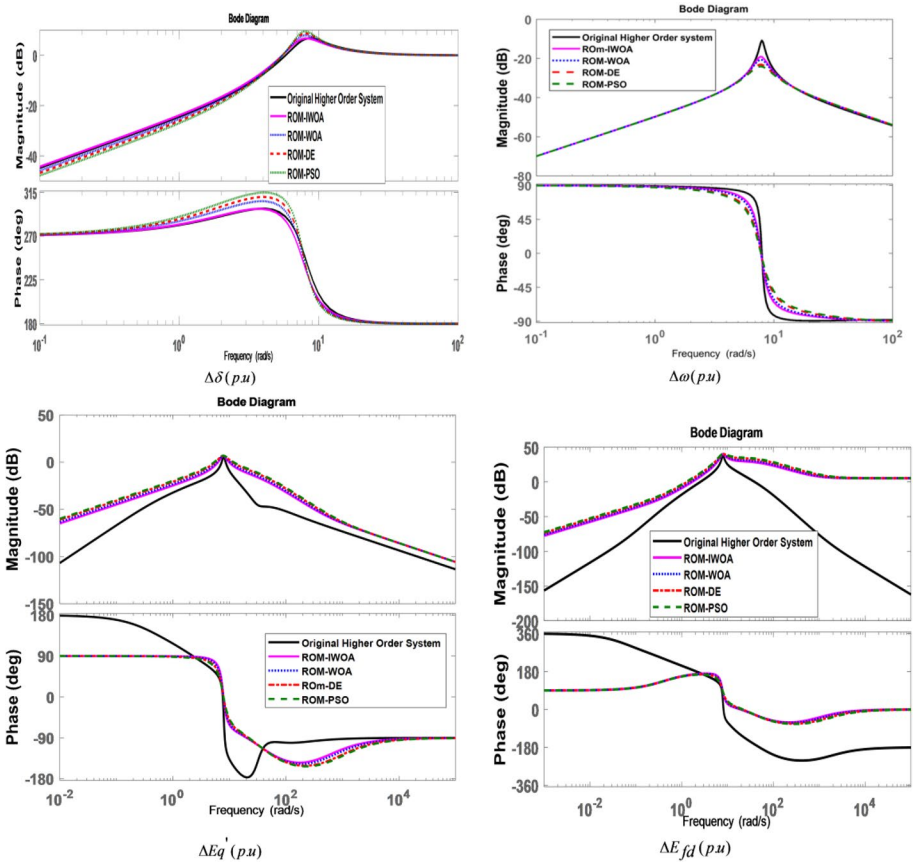

Fig. 15 Bode plot responses of loading condition 2

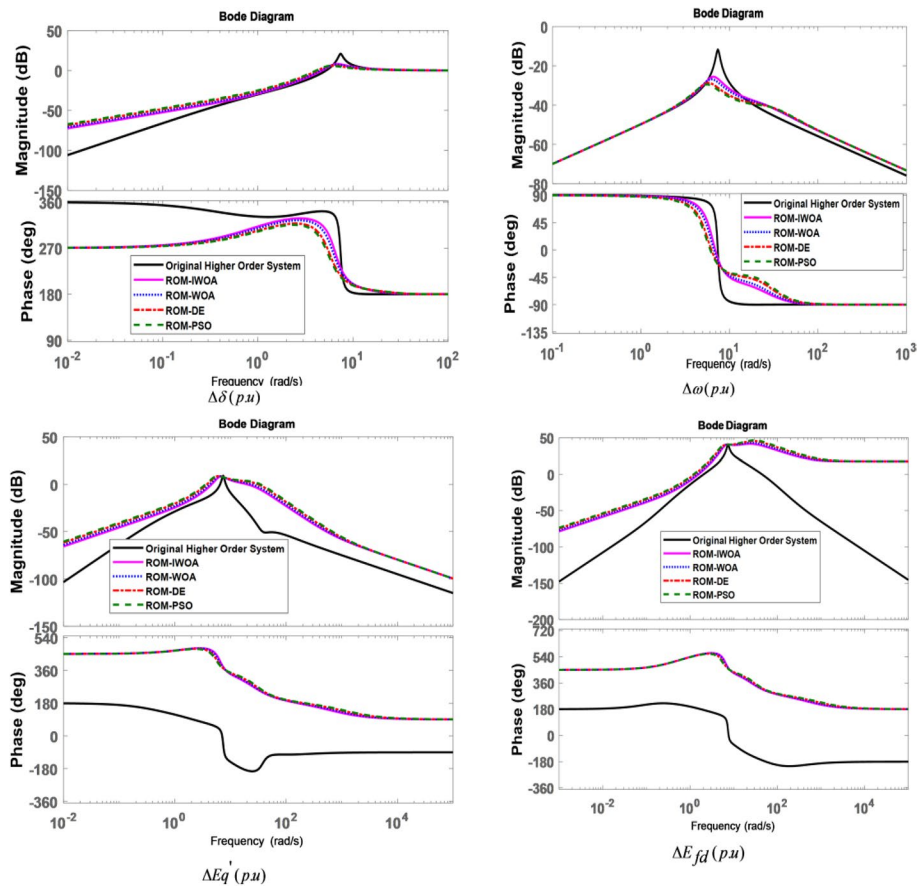

Fig. 16 Bode plot responses of loading condition 3

Appendix

State space representations of original HOSs of three operating conditions.

Operating condition 1

$$A_0 = \begin{bmatrix} 0 & 0.1 & 0 & 0 & 0 & 0 & 0 & 0 & 0 \\ -681.3 & -8.8 & -0.2 & 0 & 0 & 0 & 4.4 & 312.4 & 71.2 \\ -444.2 & 24.9 & -0.5 & 0 & 8421.1 & 8421.1 & -12.4 & -885.5 & -201.8 \\ 12.1 & 6.7 & -0.1 & -21.1 & -231.4 & 3.6 & -3.4 & -239.2 & -54.5 \\ 0 & 0 & 0 & 1.0 & 0 & 0 & 0 & 0 & 0 \\ 0 & 0 & 0 & 0 & 1.0 & 0 & 0 & 0 & 0 \\ 1.0 & 0 & 0 & 0 & 0 & -0.5 & 0 & 0 & 0 \\ 0 & 1.0 & 0 & 0 & 0 & 0 & -0.5 & -46.1 & 0 \\ 0 & 4.4 & 0 & 0 & 0 & 0 & -2.2 & -156.1 & -46.1 \end{bmatrix}; \; B_0 = \begin{bmatrix} 0 \\ 2.1697 \\ 1.4147 \\ 0.0384 \\ 0 \\ 0 \\ 0 \\ 0 \\ 0 \end{bmatrix}$$

$$C_0 = \begin{bmatrix} 314.0 & 0 & 0 & 0 & 0 & 0 & 0 & 0 & 0 \\ 0 & 0.1 & 0 & 0 & 0 & 0 & 0 & 0 & 0 \\ 0 & 0 & 0.2 & 0 & 0 & 0 & 0 & 0 & 0 \\ 0 & 0 & 0 & 0 & 8421.1 & 8421.1 & 0 & 0 & 0 \\ 0 & 0 & 0 & 0 & 8421.1 & 8421.1 & 0 & 0 & 0 \\ 0 & 1.0 & 0 & 0 & 0 & 0 & 0 & 0 & 0 \\ 0 & 0 & 0 & 0 & 8421.1 & 8421.1 & 0 & 0 & 0 \\ -12.1 & 0 & 0 & 0 & 0 & 0 & 0 & 0 & 0 \\ 0 & 0 & 0.1 & 0 & 0 & 0 & 0 & 0 & 0 \\ 0 & 19.2 & 0 & 0 & 0 & 0 & -9.6 & -648.8 & -156.1 \end{bmatrix}; \; D_0 = \begin{bmatrix} -1.000 \\ 0 \\ 0 \\ 0 \\ 0 \\ 0 \\ 0 \\ 0.0384 \\ 0 \\ 0 \end{bmatrix}$$

Operating condition 2

$$A_0 = \begin{bmatrix} 0 & 0.1 & 0 & 0 & 0 & 0 & 0 & 0 & 0 \\ -621.3 & -4.8 & -0.1 & 0 & 0 & 0 & 2.4 & 169.8 & 38.7 \\ -399.2 & -4.7 & -0.5 & 0 & 8421.1 & 8421.1 & 2.3 & 166.3 & 37.9 \\ -2.9 & 7.6 & -0.1 & -21.1 & -231.4 & 3.6 & -3.8 & -269.7 & -61.5 \\ 0 & 0 & 0 & 1.0 & 0 & 0 & 0 & 0 & 0 \\ 0 & 0 & 0 & 0 & 1.0 & 0 & 0 & 0 & 0 \\ 0 & 1.0 & 0 & 0 & 0 & 0 & -0.5 & 0 & 0 \\ 0 & 1.0 & 0 & 0 & 0 & 0 & -0.5 & -46.1 & 0 \\ 0 & 4.4 & 0 & 0 & 0 & 0 & -2.2 & -156.1 & -46.1 \end{bmatrix}; \; B_0 = \begin{bmatrix} 0 \\ 1.9788 \\ 1.2714 \\ 0.0092 \\ 0 \\ 0 \\ 0 \\ 0 \\ 0 \end{bmatrix}$$

$$C_0 = \begin{bmatrix} 314.0 & 0 & 0 & 0 & 0 & 0 & 0 & 0 & 0 \\ 0 & 0.1 & 0 & 0 & 0 & 0 & 0 & 0 & 0 \\ 0 & 0 & 0.2 & 0 & 0 & 0 & 0 & 0 & 0 \\ 0 & 0 & 0 & 0 & 8421.1 & 8421.1 & 0 & 0 & 0 \\ 0 & 0 & 0 & 0 & 8421.1 & 8421.1 & 0 & 0 & 0 \\ 0 & 1.0 & 0 & 0 & 0 & 0 & 0 & 0 & 0 \\ 0 & 0 & 0 & 0 & 8421.1 & 8421.1 & 0 & 0 & 0 \\ 2.9 & 0 & 0 & 0 & 0 & 0 & 0 & 0 & 0 \\ 0 & 0 & 0.1 & 0 & 0 & 0 & 0 & 0 & 0 \\ 0 & 19.2 & 0 & 0 & 0 & 0 & -9.6 & -648.8 & -156.1 \end{bmatrix}; \; D_0 = \begin{bmatrix} -1.000 \\ 0 \\ 0 \\ 0 \\ 0 \\ 0 \\ 0 \\ -0.0092 \\ 0 \\ 0 \end{bmatrix}$$

Operating condition 3

$$A_0 = \begin{bmatrix} 0 & 0.1 & 0 & 0 & 0 & 0 & 0 & 0 & 0 \\ -504.8 & 0.1 & -0.1 & 0 & 0 & 0 & -0.0 & -3.4 & -0.8 \\ -335.5 & 30.6 & -0.5 & 0 & 8421.1 & 8421.1 & -15.3 & -1089.5 & -248.4 \\ -20.2 & 9.2 & -0.1 & -21.1 & -231.4 & 3.6 & -4.6 & -326.7 & -74.5 \\ 0 & 0 & 0 & 1.0 & 0 & 0 & 0 & 0 & 0 \\ 0 & 0 & 0 & 0 & 1.0 & 0 & 0 & 0 & 0 \\ 0 & 1.0 & 0 & 0 & 0 & 0 & -0.5 & 0 & 0 \\ 0 & 1.0 & 0 & 0 & 0 & 0 & -0.5 & -46.1 & 0 \\ 0 & 4.4 & 0 & 0 & 0 & 0 & -2.2 & -156.1 & -46.1 \end{bmatrix}; \; B_0 = \begin{bmatrix} 0 \\ 1.6077 \\ 1.6086 \\ 0.0642 \\ 0 \\ 0 \\ 0 \\ 0 \\ 0 \end{bmatrix}$$

$$C_0 = \begin{bmatrix} 314.0 & 0 & 0 & 0 & 0 & 0 & 0 & 0 & 0 \\ 0 & 0.1 & 0 & 0 & 0 & 0 & 0 & 0 & 0 \\ 0 & 0 & 0.2 & 0 & 0 & 0 & 0 & 0 & 0 \\ 0 & 0 & 0 & 0 & 8421.1 & 8421.1 & 0 & 0 & 0 \\ 0 & 0 & 0 & 0 & 8421.1 & 8421.1 & 0 & 0 & 0 \\ 0 & 1.0 & 0 & 0 & 0 & 0 & 0 & 0 & 0 \\ 0 & 0 & 0 & 0 & 8421.1 & 8421.1 & 0 & 0 & 0 \\ 20.2 & 0 & 0 & 0 & 0 & 0 & 0 & 0 & 0 \\ 0 & 0 & 0.1 & 0 & 0 & 0 & 0 & 0 & 0 \\ 0 & 19.2 & 0 & 0 & 0 & 0 & -9.6 & -648.8 & -156.1 \end{bmatrix}; \; D_0 = \begin{bmatrix} -1.000 \\ 0 \\ 0 \\ 0 \\ 0 \\ 0 \\ 0 \\ -0.0642 \\ 0 \\ 0 \end{bmatrix}$$

Acknowledgements
Not applicable.

Author contributions
DB designed the study and formulated the objective function. DB and SM performed the simulations on test systems. SM and SR as supervisors helped in pursing the work with constructive suggestions and edited the manuscript. KRK and MKB gave technical support in improving quality of the paper. CHT and BRD have screened all the technical content. RKB, VAD, and KKKCH helped in revising the manuscript to improve the quality of the paper. All authors read and approved the final manuscript.

Funding
This work is carried out without support of any funding agency.

Availability of data and materials
Please contact author for data and material request.

Declarations

Competing interests
I admit that we have no financial and non-financial competing interests to declare.

Received: 2 August 2021 Accepted: 6 May 2023
Published online: 26 May 2023

References

1. Hutton MF, Fridland B (1975) Routh approximations for reducing order of linear time invariant systems. IEEE Trans Auto Control 20(3):329–337
2. Shamash Y (1975) Model reduction using the routh stability criterion and the pade approximation technique. Int J control 2:475–484
3. Gutman PO, Mannerfelt CF, Molander P (1975) Contributions to the model reduction. IEEE Tran Auto Control 27:475–548
4. Krishnamurthy V, Seshadri V (1978) Model reduction using the routh stability criterion. IEEE Trans Automat Contr 23(4):729–731
5. Pal J (1983) Improved pade approximants using stability equation method'. Electron Let 19(11):426–427
6. Pal J (1979) Stable reduced order pade approximants using the Routh Hurwitz array. Electron Lett 15(8):225–226
7. Bosley MJ, Lees FP (1978) A survey of simple transfer function derivations from higher order state variables. Automatica 8:765–775
8. Chen TC, Chang CY, Han KW (1980) Model reduction using the stability equation method and the pade approximation method. J Frankl Inst 309:73–490
9. Lucas TN (1979) "Optimal model reduction by multipoint pade approximation. J Frankl Inst 330(1):179–191
10. Mukherjee S, Mittal RC (2005) Model order reduction using response-matching technique. J Frankl Inst 342(5):503–519
11. Mukherjee S, Mishra RN (1987) Order reduction of linear systems using an error minimization technique. J Franklin Inst 323(1):23–32
12. Prajapati AK, Prasad R (2019) Model order reduction by using the balanced truncation and factor division methods. IETE J Res 65(6):827–842
13. Sinha AK, Pal J (1990) Simulation based reduced order modelling using a clustering technique. Comput Electric Eng 16(3):159–169
14. Vishwakarma C, Prasad R (2008) Clustering method for reducing order of linear system using pade approximation. IETE J Res 54(5):326
15. Scarciotti G, Astolfi, (2017) Data-driven model reduction by moment matching for linear and nonlinear systems. Automatica 79:340–351
16. Desai SR, Prasad RA (2013) "Novel order diminution of LTI systems using big bang big crunch optimization and routh approximation. Appl Mathemat Model 37(16–17):8016–8028

17. Sinha AK, Pal J (1990) " Simulation based reduced order modelling using a clustering technique. Comput Electr Eng 16(3):159–169
18. Parmar G, Prasad R, Mukherjee S (2007) A mixed method for large-scale systems modelling using eigen spectrum analysis and cauer second form. IETE J Res 53(2):93–102
19. Choudhary AK, Nagar SK (2019) "Order reduction techniques via routh approximation: a critical survey. IETE J Res 65(3):365–379
20. Arvind Kumar prajapathi & Rajendra Prasad (2019) Reduced order modelling of linear time invariant systems using the factor division method to allow retention of dominant modes. IETE Tech Rev 36(5):449
21. Prajapati AK, Prasad R (2022) Model reduction using the balanced truncation method and the padé approximation method. IETE Tech Rev 39(2):257–269
22. A collection of large-scale benchmark models for nonlinear model order reduction, Danish Rafiq & Mohammad Abid Bazaz, Archiv Comput Methods Eng (2022)
23. Qi J, Wang J, Liu H, Dimitrovski AD (2016) Nonlinear model reduction in power systems by balancing of empirical controllability and observability covariances. IEEE Trans Power Syst 32(1):114–126
24. Lee K, Carlberg KT (2020) Model reduction of dynamical systems on nonlinear manifolds using deep convolutional autoencoders. J Comput Phys 404:108973
25. Rafiq D, Bazaz MA (2020) A framework for parametric reduction in large-scale nonlinear dynamical systems. Nonlinear Dyn 102(3):1897–1908
26. Rafiq D, Bazaz MA (2021b) Structure preserving nonlinear reduced order modeling technique for power systems. In: 2021 seventh Indian control conference (ICC), IEEE, pp 418–423
27. Gao Z, Lin Y, Sun X, Zeng X (2022) A reduced order method for nonlinear parameterized partial differential equations using dynamic mode decomposition coupled with k-nearest-neighbors regression. J Comput Phys 452:110907
28. Pamar G, Mukherjee S, Prasad R (2007) Relative mapping errors of linear time invariant systems caused by particle swarm optimized reduced order model. Int J Comput Inform Syst Sci Eng 1(4):83–89
29. Deepa S N, & Sugumaran G (2011) MPSO based model order for- mulation technique for SISO continuous systems. "World Acad Sci Eng Technol: Int J Mathemat Comput Phys Electric Comput Eng 5(3): 288–293
30. Yadav J S, Patidar N P, Singhai J, Sidhartha Panda (2009) "Differential Evolution algorithm for model reduction of SISO discrete systems" 2009 World congress on nature & biologically inspired computing (NaBIC)
31. Sikander AA, Prasad BR (2015) A novel order reduction method using cuckoo search algorithm. IETE J Res 61(2):83–90
32. Narwal A, Prasad BR (2016) A novel order reduction approach for LTI systems using cuckoo search optimization and stability equation. IETE J Res 62(2):154–163
33. Sambariya D K and Arvind G (2016) "Reduced order modelling of SMIB Power System using Stability equation method and firefly algorithm." In: 2016 IEEE 6th international conference on power systems (ICPS),1–6 - 2016, New Delhi
34. Lavania S, Nagaria D (2016) BAT algorithm for model order reduction. Int J Mathemat Model Numer Opt 7(3–4):244–258
35. Jain S, Hote Y, Saxena S (2020) Model order reduction of commensurate fractional-order systems using big bang – big crunch algorithm. IETE Tech Rev 37(5):453
36. Vasu G, Sivakumar M, Ramalingaraju M (2020) Optimal model approximation of linear time- invariant systems using the enhanced DE algorithm and improved MPPA method. Circuits Syst Signal Process 39:2376–2411
37. G, V., M, S. and M, R. (2021) Optimal IMC-PID controller design for large-scale power systems via EDE algorithm-based model approximation method. Trans Inst Meas Control 43(1):59–77
38. Vasu G, Sivakumar M, Ramalingaraju M (2020) A novel model reduction approach for linear time-invariant systems via enhanced PSO-DV algorithm and improved MPPA method. Proc Inst Mech Eng Part I: J Syst Control Eng 234(2):240–256
39. Mafarja MM, Mirjalili S (2017) "Hybrid whale optimization algorithm with simulated annealing for feature selection. Neuro Comput 260:312
40. Mirjalili S, Lewis A (2016) The whale optimization algorithm. Adv Eng Softw 95:51–56
41. Sambariya K, Sharma AK, Gupta T (2019) Order reduction of air core transformer using continued fraction method. J Eng Sci Technol 14(1):253–264
42. Vishwakarma CB, Prasad R (2019) clustering method for reducing order of linear system using pade approximation. J Eng Sci Technol 14(1):2019
43. M.srinivasan, A.krishnan, (2010) " Transformer linear section model order reduction with an improved pole clustering. Eur J Sci Res 44(4):541–549
44. Parmar G, Prasad R, S. mukkherjee, (2019) "A mixed method of large scale systems modeling using eigen spectrum analysis and cauer second form. IETE J Res 53(2):93–102
45. Shamash Y (1975) Model reduction using the routh stability criterion and the pade approximation technique. Int J Control 21:475–484

Publisher's Note

Springer Nature remains neutral with regard to jurisdictional claims in published maps and institutional affiliations.